Scientific Research Publishing

Open Journal of Geology, 2023, 13, 623-650
https://www.scirp.org/journal/ojg
ISSN Online: 2161-7589
ISSN Print: 2161-7570

Spatial Analysis of Gravity Data in the Basement of the Yaoundé-Yoko Area from the Global Gravity Model: Implication on the Sanaga Fault (South-Cameroon)

Mouzong Pemi Marcelin[1*], Ngatchou Evariste[2], Njiteu Cyrille Donald[1], Cheunteu Fantah Cyrille Armel[3]

[1]Technology and Applied Sciences Laboratory, Department of Basic Sciences, University Institute of Technology, University of Douala, Douala, Cameroon
[2]Highter Teacher Training College, University of Yaoundé I, Yaoundé, Cameroon
[3]Laboratory of Geophysics and Geoexploration, Department of Physics, The University of Yaoundé I, Yaoundé, Cameroon
Email: *mouzong2002@yahoo.fr

How to cite this paper: Marcelin, M.P., Evariste, N., Donald, N.C. and Armel, C.F.C. (2023) Spatial Analysis of Gravity Data in the Basement of the Yaoundé-Yoko Area from the Global Gravity Model: Implication on the Sanaga Fault (South-Cameroon). *Open Journal of Geology*, **13**, 623-650.
https://doi.org/10.4236/ojg.2023.137027

Received: April 20, 2023
Accepted: July 3, 2023
Published: July 6, 2023

Abstract

In this work, gravity anomalies from the XGM2016 global gravity model are used to study the basement of the Yaounde, Yoko area. The aim is to locate the characteristic tectonic faults and to characterize the geometry of the basement of these localities in order to improve the knowledge of the structural and tectonic basement of the study area. Numerical filters (vertical gradient, horizontal gradient, upward continuation) and Euler deconvolution were applied to the gravity anomalies respectively for qualitative and quantitative analysis. The results of the qualitative analysis allowed us to establish the lineament map of the study area; ranging from 0 to 35 km depth. For the quantitative analysis, the work is done in two parts: 1) highlighting the distribution of depths of geological structures in the basement of the study area; 2) 2D1/2 modeling of geological structures to highlight the geometry of the basement of Yaounde, Yoko area. Thus, from five suitably selected profiles, the established models reveal the presence of eight blocks of geological structures of different densities and analyze their implications on the Sanaga Fault. Moreover, the models show that the positive anomalies characteristics for the Sanaga Fault reflect the anomalous character due to the strong dominance of the shale intrusion in the basement.

Keywords

Gravity Anomalies, Global Gravity Model, Basement, Lineaments, Numerical

Filters, Modeling

1. Introduction

The knowledge of the structure of the earth requires both surface and deep studies. Thus, thanks to geophysical methods, it is possible to investigate the basement at depth and explore hidden areas in order to have a picture of the deep structure of the globe. Geophysics, known as a discipline of the physics of the earth's environment, was first developed in the field of prospecting and then for the fight against environmental hazards on land.

In Cameroon, the structural context consists mainly of four sets: the Kribi-Campo Fault (KCF), the Tcholliré Banyo Fault (TBF), the Cameroon Central Shear (CCC) and the Sanaga Fault (SF) [1] [2]. In addition, the Sanaga Fault represents one of the major dextral mylonitic shear zones crossing Cameroon from northeast to southwest [1] [3] [4]. The Sanaga Fault [5], a SW-NE trending shearing fault that operated as a dextral strike-slip, which extends from Edea to the west, is the Cameroonian extension of the Bozoum-N'dele Fault [3] and may be the southern limit of the dextral strike-slip of the Pan-African Belt with respect to the portion of the Congo Craton located in Cameroon [5]. A little further south in Cameroon, the Abong-Mbang-Akonolinga tectonic corridor illustrates the cumulative characteristics of brittle and tangential tectonics [6]. Thanks to the work on the global structuring of the tectonic faults of Cameroon, it is now known that the basement of Cameroon has been affected by several geodynamic phenomena [7]. Thus, the geodynamic structural context of the Abong-Mbang-Akonolinga fault has been revealed as being that of a collision chain between the Congo Craton to the south and the Adamawa-Yadé domain [2] [8], which may be at the origin of the Sanaga Fault.

In this work, we conduct a geophysical investigation using data from the XGM2016 global gravity model for a structural analysis of the Yaounde, Yoko area in Cameroon. The unavailability of gravity data suggested the choice of this method. For the analysis, we put an emphasis on two points: 1) the understanding of the geological parameters of the study area; and 2) identifying tectonic faults aids in finding mineral-rich areas for energy solutions for the exploitation of basement mineral resources with regard to energy challenges. To achieve the objectives, we exploited the geological setting of the study area, and adopted a data processing methodology based on the use of digital filters for qualitative and quantitative analysis.

2. Geological and Tectonic Setting

Central Africa is essentially made up of a Precambrian basement comprising magmatic and metamorphic rocks subdivided into several geological periods from Cameroon to Sudan [3] [9]. The outcropping rocks are mainly granites and

migmatites rejuvenated during the Pan-African episode [3]. For the study area, we have two main structural units: the northern termination of the Congo Craton (stable and Archean in age, 2000 Ma) and the North Equatorial Pan-African Range including the Sanaga Fault [10]. Three Craton blocks that were not affected by the past Pan-African orogeny are well located in Africa (**Figure 1(a)**) with geological structures dating from the Precambrian [11]. These are the West African Craton (WAC), the Kalahari Craton (KC) and the Congo Craton (CC) and a Meta-Craton outcropping in the northern part of Cameroon [11]. In southern Cameroon, the northern limit of the Congo Craton (CCL) is located [7]. This Craton occupies most of Central Africa [10]. In Cameroon, the Ntem Group and its Proterozoic cover constitute its northern termination. It contains the Ntem, Ayina and Nyong units and includes a set of gneiss-granulites that form the banded series and the ferriferous furrows that are greenstone belts [12] [13] [14]. In the Pan-African Belt, it occupies most of the Cameroonian lithosphere.

The Pan-African is a major tectonic episode that marked the African continent

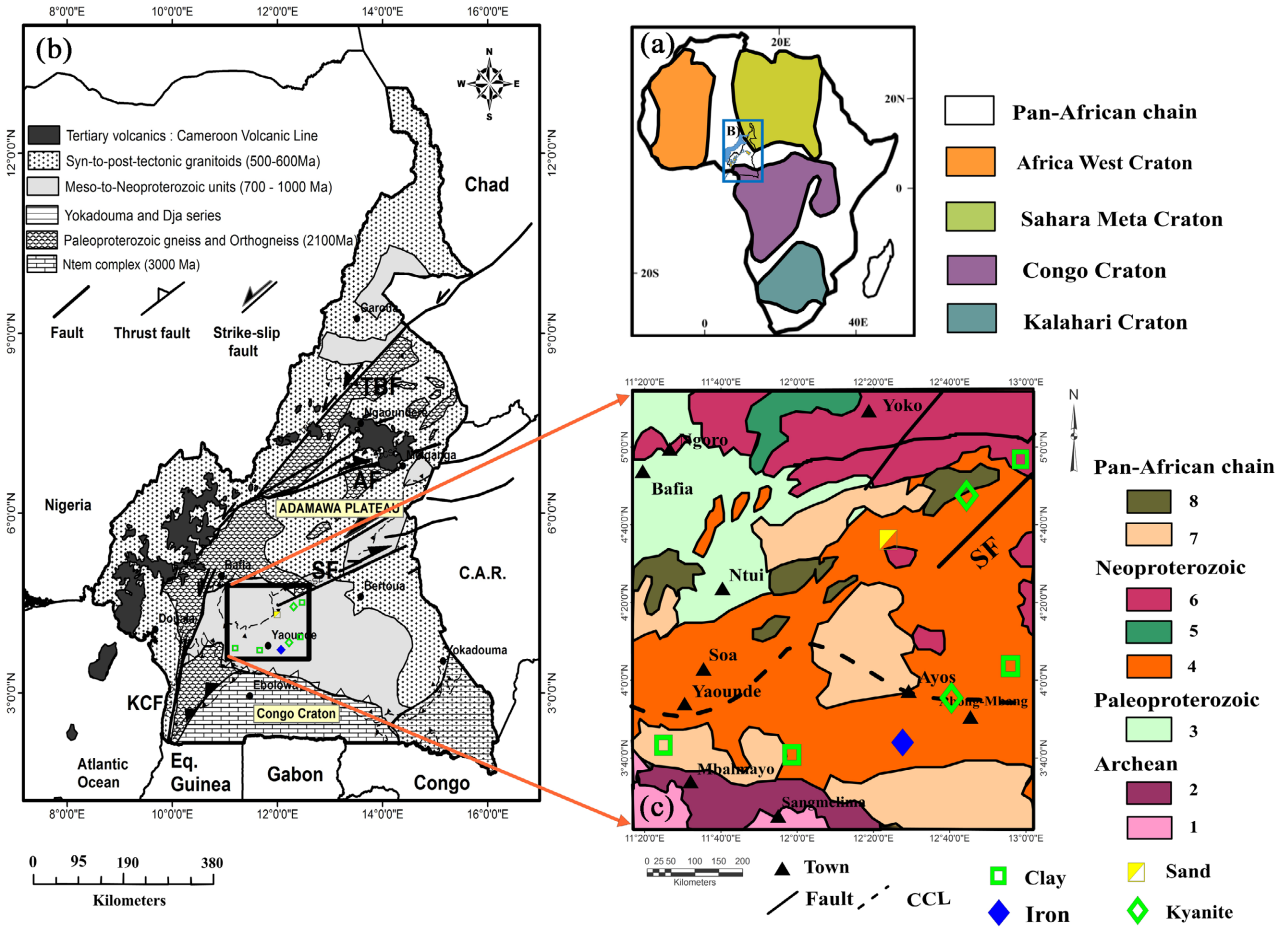

Figure 1. (a) Africa Craton [11]; (b) Cameroon geological map [2]. (c) Geological map of study area (extraded of geological map of Toteu [15]), with Congo Craton Limit (after Cheunteu [7]), 1. Gneiss granulitic, Meso-Archean, 2. TTG no charnockitic, Meso-Archean, 3. Gneissic complex, 4. Gneiss and micaschists, 5. Granitoids Post-tectonic, 6. Granitoids Syn-at tardi-tectonic, 7. Schists, Group Yaounde, 8. Quarztits, Group Yaounde.

and covers a period from 1000 Ma to 500 Ma. The formations encountered form a vast and complex network of orogenic domains [15]. The North Equatorial Pan-African Belt constitutes the most of the basement and outcrops in Cameroon (**Figure 1(b)**). The formations encountered cover several groups, namely: 1) the Yaoundé series, which contains mainly granulites of plutonic origin with the presence of syn-metamorphic igneous rocks in the vicinity and in the city of Yaoundé [4]; 2) the Ayos-Mbalmayo-Bengbis (AMB) series along the northern edge of the Ntem Group, which is continuous with the garnet-bearing micaschists of the Yaoundé series. It consists essentially of schists and micaschists [16].

In the study area, several geological structures abound in the subsurface (**Figure 1(c)**) ranging from Archean (Granulitic Gneiss and TTG no charnockitic, Meso-Archean) to Neoproterozoic (Gneiss and micaschists, Granitoids Post-tectonic and Granitoids Syn-at tardi-tectonic); as well as the markings of a few structural features (**Figure 1(c)**) such as the localized fault in the northeastern part of the study area. This dense fracture is considered to mark an important lineament that we will refer to as the Sanaga Fault. North of the Sanaga Fault, the structural lines in the quartzites are fine, regular and thus provide some good structural markers [5]. The Sanaga Fault separates two major outcrop zones: (Series 1) Lom in the north and (Series 2) Nanga-Eboko in the south [17]. The Sanaga Fault completes the Central African lineament bundle described by [3] to the west. It extends the Bozoum-N'dele accident westward, forming the Sanaga-N'dele feature, the longest and most rectilinear of the Adamawa axis lineaments [5].

3. Data used

In this work, we use data from the global gravity model (XGM2016) to highlight Bouguer anomalies at the spherical harmonic degree of 719. The model development utilized altimetry, onboard and airborne ground data, and topography datasets [18]. Data collection was carried out by satellites such as GRACE, GOCE, and LAGEOS. The topographic potential models incorporated in the study represent the gravitational potential resulting from the attraction of Earth's topographic masses. It's important to note that the gravity values in the models are predicted rather than actual. The accuracy of these predictions depends largely on the resolution and precision (errors) of the numerical model. The data grid of this gravity model has been extracted from the ICGEM (International Centre for Global Earth Models) website (http://icgem.gfz-potsdam.de/calcgrid) with a resolution of $0.1^{\circ} \times 0.1^{\circ}$. These data were corrected using the tesseroid method [19] with a homogeneous density distribution. For the calculation, 2670 $kg.m^{-3}$ were used as the average value of the density of the upper continental crust [20] gravity and bathymetric corrections were calculated for a seawater density model [21] [22] [23] [24] as a function of depth. These data are used in this work to characterize the subsurface of the Yaounde - Yoko localities.

4. Methodology

In this study, gravity anomaly processing methods were used for a structural characterization of Yaounde - Yoko basement and to highlight not only the characteristic tectonic faults [25] [26] [27] [28] but also to characterize the basement geometry of these localities and its surroundings. For the methodology, the filters used are described below. The processing methodology consists of two phases. In the first phase, a qualitative analysis of Bouguer anomalies was conducted to examine the distribution of anomalies and their gradient contrasts. This involved applying upward extension filters, vertical gradients, and horizontal gradients [7]. Since the study focuses on the Yaoundé-Yoko basement structure, a multi-scale analysis of these digital filters was performed to understand their behavior with depth and to combine structural characterization [7]. In the second phase, the geometry of the study area's basement was characterized. This involved mapping the spatial distribution of geological structure depths and developing a 2D1/2 model to comprehend the geodynamic context in relation to the region's lineament orientation [7].

4.1. The upward Continuation

In order to study the behavior of geological structures and their formation processes, we perform a multiscale analysis of gravity anomalies in the study area including Yaounde and Yoko in Cameroon. The upward Continuation is a method that uses the low-pass filter operator by attenuating the high frequencies of the fields associated with the effects of the surface gravity structures, thus highlighting the anomalies of the deeper structures, as a function of the altitude of the extension [29]. In the frequency domain, the expression of the upward extension operator for a map is defined by relation (1):

$$L(r) = \mathrm{e}^{-k\Delta z} \tag{1}$$

where k is wavenumber and z the variation of depth.

4.2. The Horizontal Gradient of Bouguer Anomalies

The horizontal gradient (HG) is a method used to locate lateral contacts of geological structures in the basement. It allows to highlight areas with a strong gravity gradient contrast [24]. It is favorable for the study of different deep discontinuity zones in order to give their tectonic implication. In the spatial domain, the horizontal gradient (HG) of a potential field $g(x,y)$ of the seam along the x and y plane is given by the relation (2) [25]:

$$g_{DH} = \sqrt{\left(\frac{\partial g}{\partial x}\right)^2 + \left(\frac{\partial g}{\partial y}\right)^2} \tag{2}$$

where $\frac{\partial g}{\partial x}$ and $\frac{\partial g}{\partial y}$ are respectively the derivatives following x and following y of the field g.

The x component of the gradient emphasizes the discontinuities and direction of the contacts while the y component acts in a similar way to the direction perpendicular to x.

4.3. The Vertical Gradient of Bouguer Anomalies

In general, the derivation operators performed on the anomaly maps are intended to attenuate or, on the contrary, enhance certain information contained in the potential field data [7]. The vertical derivation operator acts as a high-pass electronic filter by amplifying short wavelengths, thus highlighting anomalies associated with shallow structures at the expense of those associated with deep structures [7] [25] [29]. The horizontal gradient (DH) of a potential field $g(x,y)$ is calculated by relation (3) from [30]:

$$g_{Dv} = \left(\frac{\partial P}{\partial z}\right)_h \tag{3}$$

where P is the potential field and h is the height.

4.4. Multiscale Analysis of Gradient Maxima from Gravity Data

The upwards continuation map of Bouguer anomalies at different altitudes (**Figure 3**) allowed us to differentiate anomalies related to regional (deep) structures from those originating from local (shallower or superficial) structures. The horizontal gradient map highlights areas with steep density variations, inter-perceived either as faults or geological contacts, or as intrusive formations [7] [31]. Multiscale analysis of the horizontal gradient involves coupling the horizontal gradient to the upward continuation at different height [32]. The maxima of the horizontal gradient are determined by the method of [26].

The analysis methodology consists of mapping the continued upward field at different height with a constant step size; then for each map, the horizontal gradient maps are constructed. These horizontal gradients are used to locate maxima, and finally to map the maxima of the gravity data. The approach of automatically locating horizontal gradient maxima [26] was utilized. The process involved two steps. In the first step, Bouguer anomalies were extended from 0 km to 40 km at a consistent step size. In the second step, the horizontal derivative (HD) was computed for each upward continuation anomaly map, and the gradient maxima were determined for each extended horizontal derivative map. To locate these maxima, a regular grid was defined, comparing the value of the center node within a 3 x 3 window to its four neighboring grid points [7] [26].

4.5. Euler Deconvolution Method

The Euler deconvolution filter has been applied to gravity anomalies of Yaounde, Yoko area in Sud-Cameroon. Euler deconvolution allows the precise location of the depths of potential field anomaly sources in the basement. The Euler deconvolution technique uses first order x, y and z derivatives to determine the location and depth of various targets (sphere, cylinder, dyke and contact); each cha-

racterized by a specific structural index. The Euler homogeneity relation for gravity data is defined by relation (4) [33].

$$\left(x-x_0\right)\frac{\partial M}{\partial x}+\left(y-y_0\right)\frac{\partial M}{\partial y}+\left(z-z_0\right)\frac{\partial M}{\partial z}=N\left(B-M\right) \tag{4}$$

where (x_0, y_0 et z_0) is the position of the gravity source whose total field (M) is detected in (x, y, z), B the regional potential field, and N the degree of homogeneity as the structural index. The structural index (N) depends on the geometry of the source (**Table 1**) and characterizes the rate of change of the intensity of the anomaly with distance [34]. Another parameter that comes into play for the determination of adequate solutions is the choice of the window size [35], who noted that the appropriate choice of the window size depends on the wavelength of the anomaly examined and the grid pitch. The tolerance (Z) representing the error on the depth determination is taken into account known as the solution acceptance rate [35]. The quality of this evaluation depends largely on the appropriate choice of the structural index, which is a function of the geometry of the causal bodies [36]. To characterize the subsurface of the study region using Euler deconvolution, we initially utilized the Bouguer anomalies from the global gravitational model to determine spatial anomaly contrasts in the x, y, and z directions. Next, we established a method for calculating the depths of geological structures. This involved defining parameters such as a window size of 15 km × 15 km, a structural index of 0, and a tolerance of 10% for depth estimation. The selection of the window size was adjusted to determine the display dimensions of the spatial distribution.

4.6. 2D1/2 Modeling of Gravity Data

In order to describe the subsurface geometry of the Yaounde-Yoko region, 2D1/2 modeling was adopted in this work. The 2D1/2 modeling was previously proposed in gravimetry by Cady [38]. The principle of modeling allows for less important ratios of main elongation to transverse extension, to take into account the limit length of the body [39]. The 2D1/2 modeling was performed by selecting specific profiles to extract the gravity anomalies for modeling purposes. The approach involved adjusting a theoretical curve to match the experimental curve of Bouguer anomalies. The initial model was established based on surface geological observations [40]. The final model comprised adjacent polygons with constant density, aiming to generate a modeled curve that closely matched the

Table 1. Structural index for magnetic and gravity sources [33] [34] [37].

Source	structural index
Contact	0
Vertical Dyke et sill	0
Vertical cylinder and pipe	1
Sphere	2

observed values in terms of gravity effects [40]. The most valid model was determined by assessing the correlation between the theoretical curve and the observed data, while also considering geological constraints [40] [41].

5. Results and Interpretations

5.1. Bouguer Gravity Data

The result of the analysis and processing of data from the global gravity model (XGM2016) led to the Bouguer anomalies (**Figure 2**) compiled to highlight Bouguer anomalies with respective interval contours of 5 mGal. It highlights the distribution of density anomalies of geological structures and contains information on discontinuities present in the subsurface, which can be highlighted from the gradient filters. The qualitative interpretation allows us to divide the area into three zones: 1) anomalies positives area, located in the center with an extension in the northeast direction towards Adamawa, to the east a little north of Abang-Mbang and to the northwest near Bafia and Ngoro; 2) anomalies negative area, located in the south and southeast of the study area. According to the geology, these negative anomalies are mostly located on metamorphic rocks such as schists. These geological structures are also located around Yaounde and

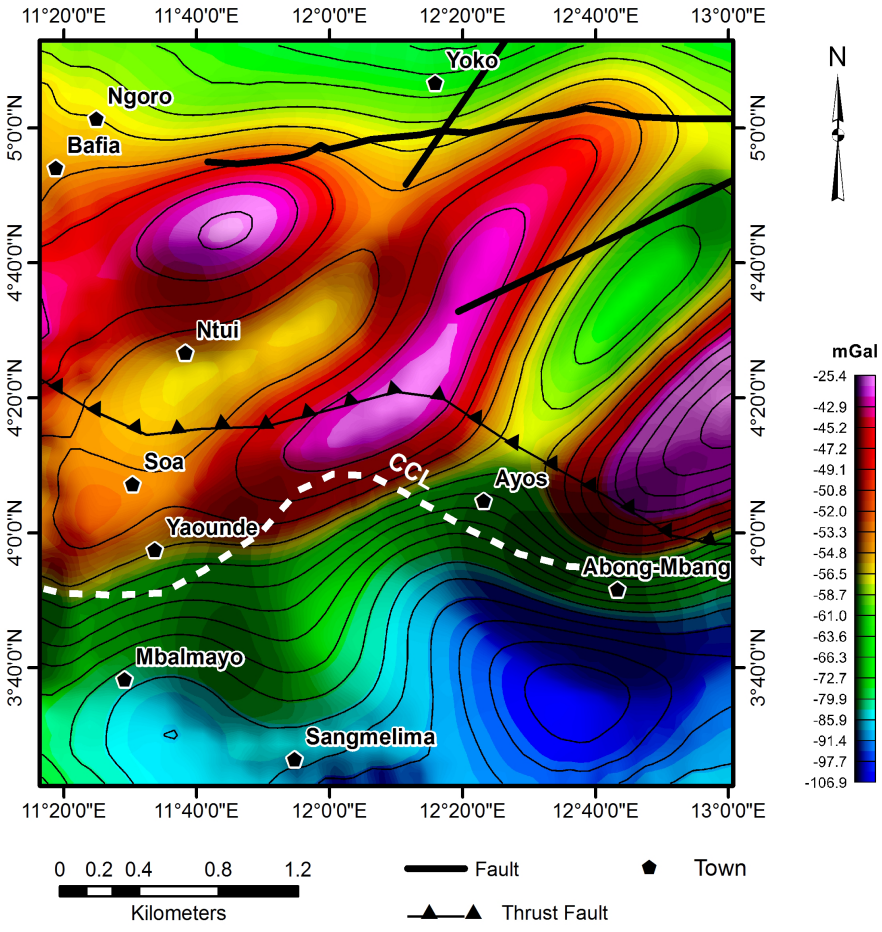

Figure 2. Complete Bouguer anomalies at the spherical harmonic degree of 719 map.

Mbalmayo and in the Ayos locality. This could be considered as the intrusion of schists in the investigation area. 3) the gradient areas; the first following the East-West direction from Abang-Mbang to Yaounde located on the schists and Gneiss of the Meso to Neoproterozoic unit; the second in the North-East of circular shape located on the schists and Gneiss of the Meso to Neoproterozoic unit and Gneiss - Orthogneiss of the Paleoproterozoic.

Bouguer gravity perturbations vary mainly in the range of −106.9 to −25.4 mGal. The negative values in the study area are located on the northern portion of the Congo Craton. While the strong predominance of positives values is found on the NE-SW trending Pan-African belt. Bouguer gravity perturbations are strongly spatially correlated with crustal thickness variations and deeper lithospheric structures. Gravity troughs on the Bouguer Congo Craton reflect either regional Moho or granite batholiths that may be due to isostatic compensation of major topographic features. In addition, the NE-SW gradient contrasts may reflect the existence of the Sanaga Fault already highlighted by [2].

5.2. Upward Continuation of Bouguer Anomalies

In this section, we use the low-pass numerical filter for a multiscale analysis of the Bouguer anomalies in order to study the behavior of the anomalies of the subsurface geological structures of the study region with depth. Analysis of the spatial behavior of anomalies and depth shows the influence of the deep structures and the contribution of the different formations to the evolution of the North Equatorial Pan-African Range and the Congo Craton.

Thus, on the Bouguer anomaly map, two major axes of high amplitude anomalies are located along the ENE-WSW and NE-SW directions representing respectively the Ntui anomaly and the Sanaga fault. A little further south, gradient contrasts of almost E-W direction are located and mark the northern transition zone between the Congo Craton and the Pan-African Belt. This Bouguer anomaly map has been extended upwards to altitudes of 5 km, 10 km, 20 km, 30 km and 45 km. Analysis of these maps show that the two main axes of positive amplitude of the Bouguer anomalies progressively fade with depth towards the west and northwest. It is easy to see that the positive anomaly that characterizes the Sanaga Fault fades and disappears at 30 km (**Figure 3**). This suggests that these anomalies may have an intracrustal origin. The Bouguer anomalies thus highlighted, translate here the anomalous character of the densities due to the heterogeneity of the geological structures in the crust of the investigated region. These anomalies observed could be the consequence of geodynamic phenomena among which the continental collision between the Pan-African Belt and the Congo Craton according to [2].

5.3. Horizontal Gradient of Bouguer Anomalies

The horizontal gradient map of Bouguer anomalies in the study area shows horizontal contrasts of high and low density amplitudes of various shapes (**Figure 4**).

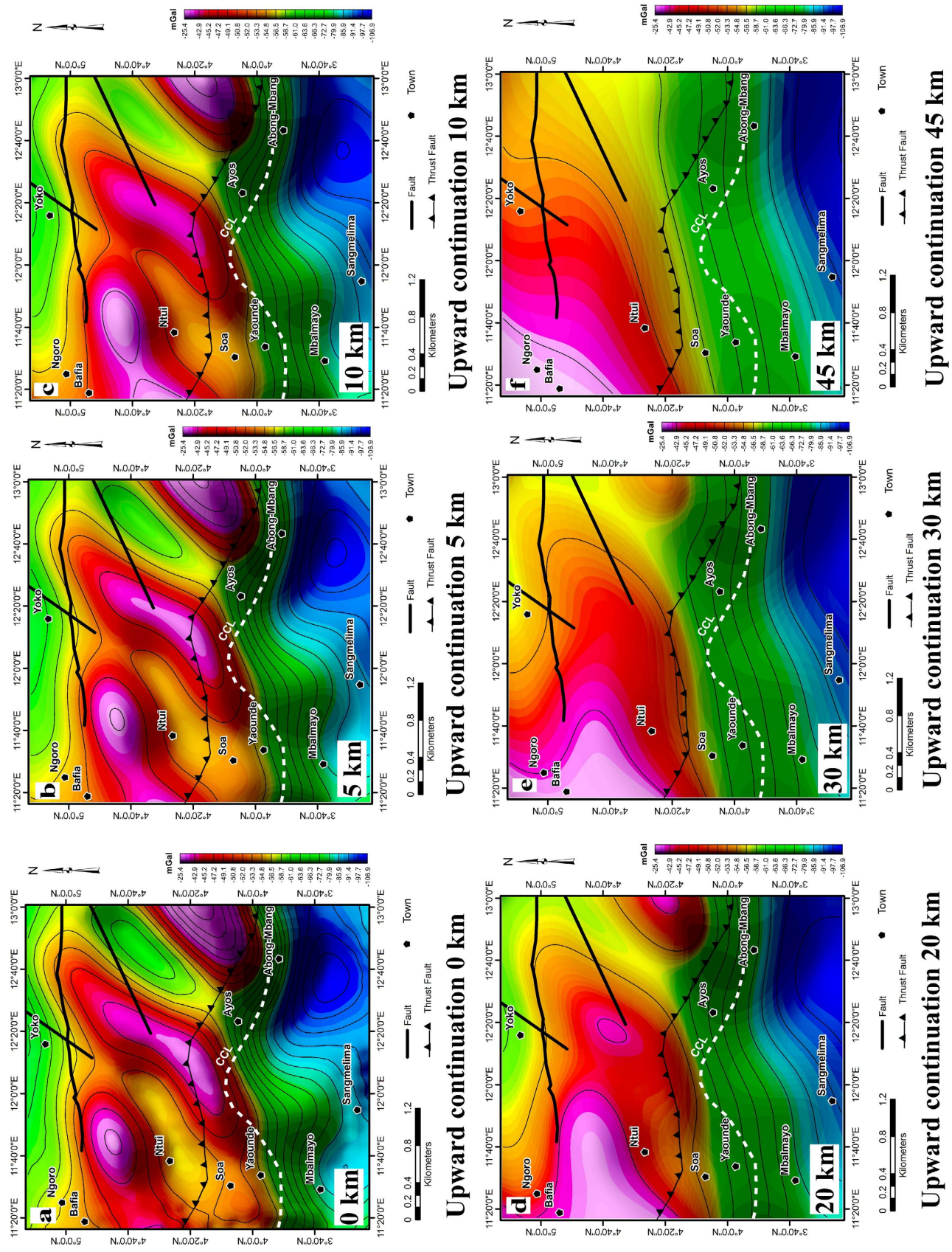

Figure 3. Upward continuation of Bouguer anomaly map at 5 km, 10 km, 20 km, 30 km and 45 km.

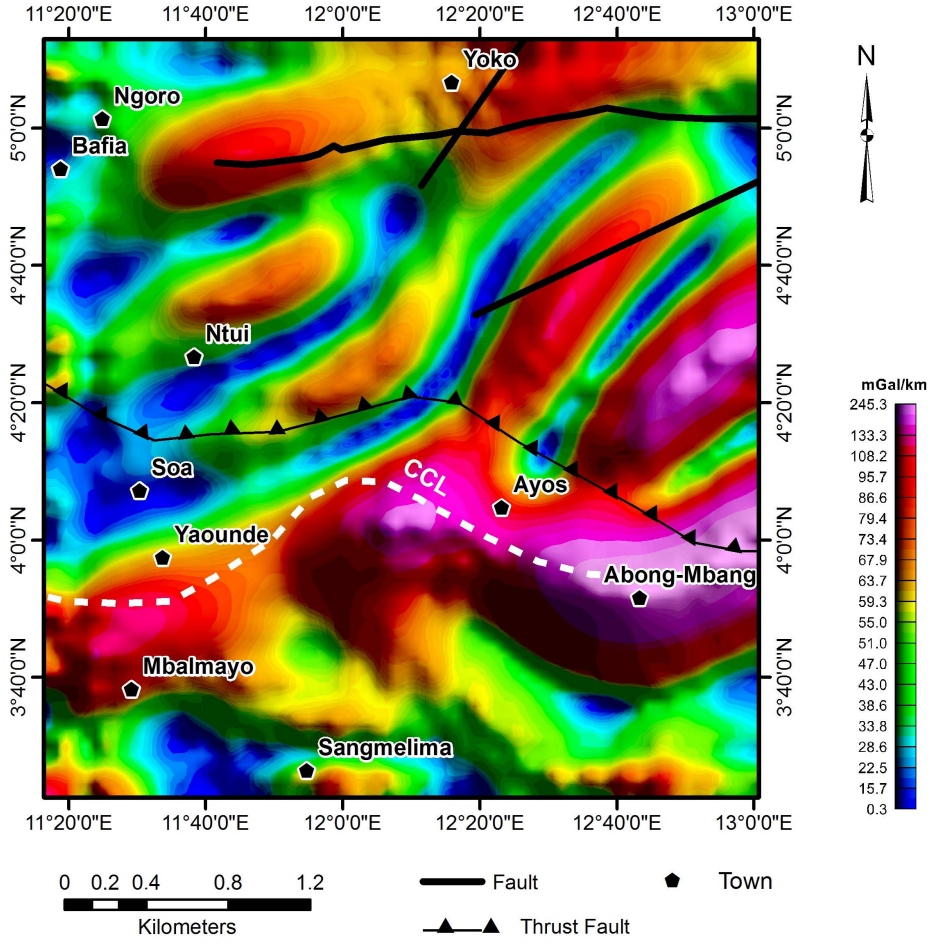

Figure 4. Horizontal gradient of Bouguer anomalies map.

The strong density gradients are observed in area such axis as Mbalmayo, Yaoundé, Ayos and Abang-Mbang. These horizontal gradients likely represent the northern edge of the Congo Craton with the Pan-African Belt in the study area [7]. The strong deformation of this boundary almost in the center of the map suggests the presence of a thrust from the geological structures of the Congo Craton on the Pan-African Belt. This area (**Figure 4**) is the area where the horizontal gradient contrasts of the northern edge of the CC meet those of the NE-SW oriented Pan-African belt, marking the path of the Sanaga Fault.

Moreover, in the Yoko locality, positive gradient amplitudes are highlighted. These gradient contrasts are less significant than those located in Yaounde, Ayos and Abong-Mbang. Overall, the qualitative analysis of the horizontal gradients shows us the extent to which the subsurface of the investigation area is highly rugged; the presence of these lineaments, albeit widely spaced due to the resolution limitations of the XGM 2016 global gravity model data, serves as evidence that the subsoil of the study area is significantly influenced by geodynamic phenomena. This highlights the need for careful investigation to understand the underlying causes responsible for these geological features.

5.4. Vertical Derivative of Bouguer Anomalies

The first vertical derivative map for Bouguer anomaly values illustrates the prevalence of sharper contacts of gravity ripples (Figure 5). They highlight the presence of tectonic faults, intrusions and very important surficial geological contacts in the subsurface of the study area. These very short wavelength structures are clearly visible within the gravity field anomaly groups. An analysis of the map shows that the vertical gradients located in the Yaoundé, Ayos and Abang-Mbang localities could materialize the boundary between the northern edge of the Congo Craton and the Pan-African Ridge. This could confirm the termination of the Sanaga Fault at the boundary of the Northern edge of the Congo Craton in Southern Cameroon.

5.5. Multiscale Analysis of Bouguer Anomalies Horizontal Gradient Maxima

In this work, the localized maxima for each anomaly depth were superimposed (Figure 6) for the lineament plot (Figure 7). Therefore, the lineaments can be considered as a succession of characteristic lineaments that may be related to the trend of existing faults in the study area [7] [31] [42].

Application of this method to Bouguer anomaly maps shows that superimposed

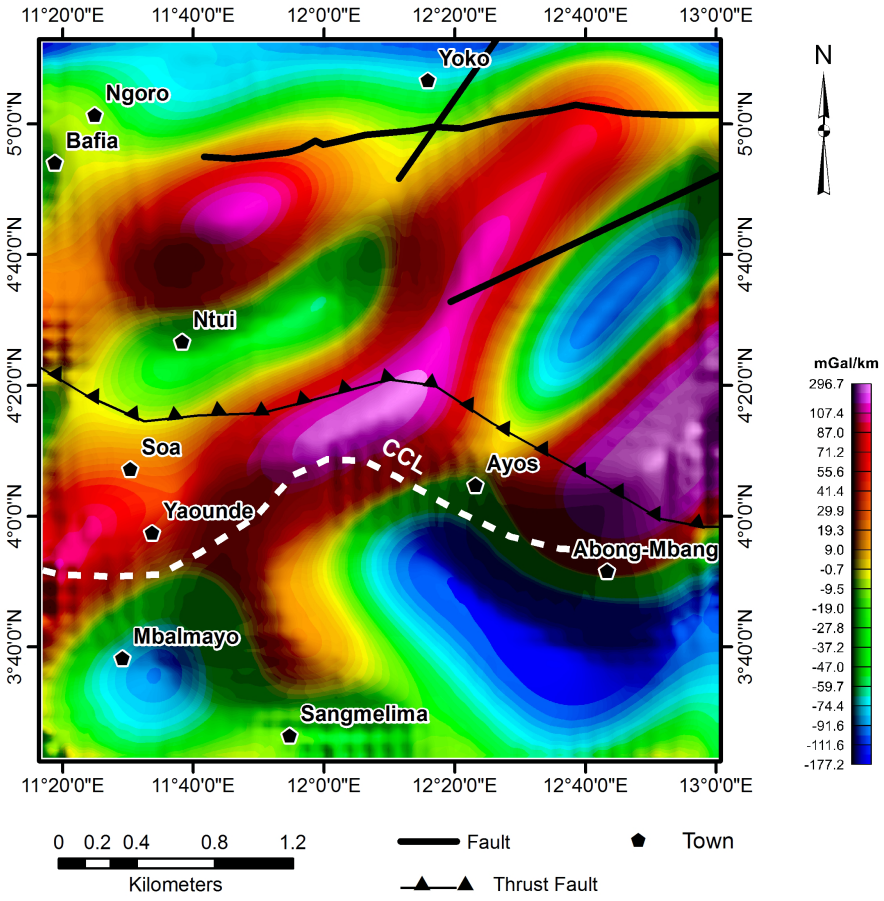

Figure 5. Vertical gradient of Bouguer anomalies map.

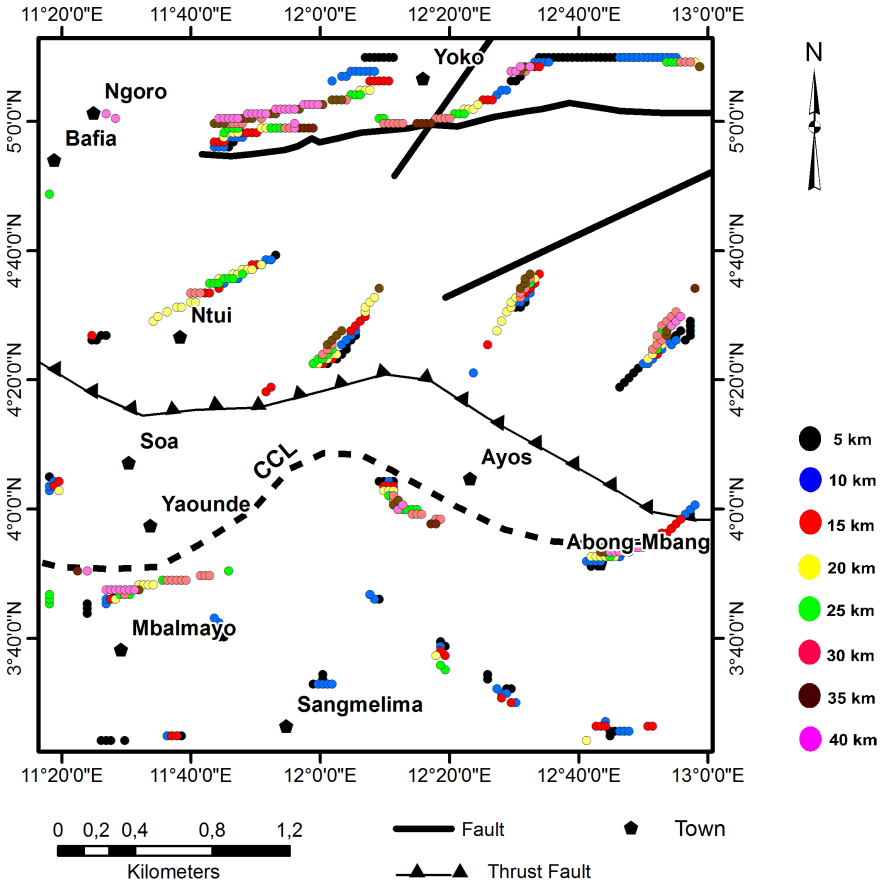

Figure 6. Maxima of horizontal gradients of Bouguer anomalies map.

local maxima form narrow ripples above abrupt changes in density. The behavior and directions of the superimposed maxima give us information about the orientation and dip of the localized lineaments (**Figure 6**). The distribution of maxima along the quasi-linear gradient shape can be interpreted as the intracrustal density change [7] [43].

5.6. Mapping of Gravity Lineaments

The superposition of the maxima (**Figure 6**) obtained from the multiscale analysis of gravity anomalies and superimposed on the gradient contrasts has allowed us to highlight the tectonic faults contained in the subsurface of the lithosphere in Cameroon (**Figure 7(a)** & **Figure 7(b)**). The results obtained from the processing of gravity anomalies in the study area confirm and clarify the pattern of tectonic structures recognized by geological studies [2] [10]. **Figure 7(a)** & **Figure 7(b)** illustrates the main boundaries between zones that exhibit a significant density contrast. Among these identified fault segments are the faults (L1, L5, L8, L15 and L12) running from Abang-Mbang to Ayos with an extension into the Yaounde locality; considered as the lineaments of the northern edge between the Congo Craton and the Pan-African Belt.

This transition zone has in the past been highlighted through studies on

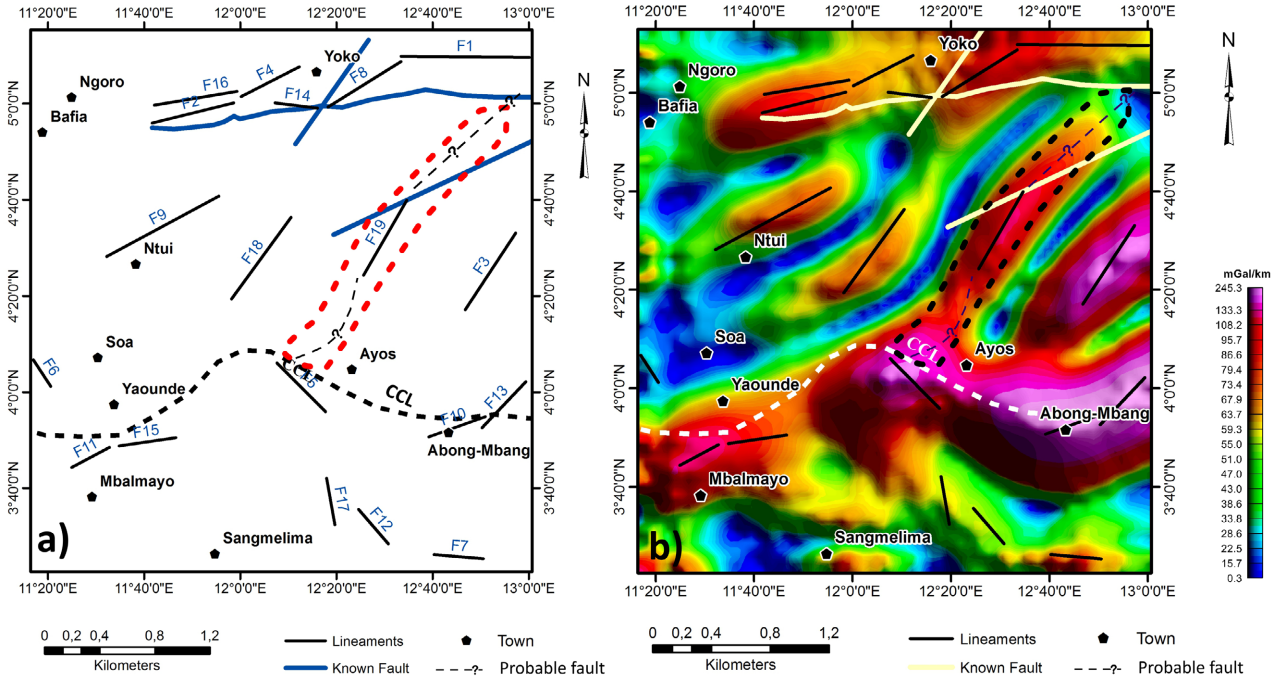

Figure 7. (a) Lineaments of Bouguer anomalies map; (b) lineaments superimposed on the horizontal gradient.

lineament mapping in Cameroon [7] [43] [44] and gravity imaging of crustal structures and their implications for tectonics in the same region [43] using gravity data. The orientation of the highlighted lineament networks is determined by the orientation of local maxima that are overlaid with depth information. These lineaments have been listed in **Table 2** with their different orientations.

5.7. Euler Deconvolution of Gravity Data

For the determination of the depths of the geological structures in our study area, the Euler deconvolution method was used to determine the depths of the geological structures in the subsurface of the study area (**Figure 8**). According to the Bouguer anomaly map, two zones of strong anomaly contrasts are located in the E-W and NE-SW directions, corresponding respectively to the northern edge of the Congo Craton and the Sanaga fault.

The low-pass filter was applied to the Bouguer anomalies in order to attenuate the high frequencies due to surface sources to a depth of 45 km. The anomalies obtained at this depth were considered in this study as regional anomalies; we then extracted these anomalies from the gravity field to highlight the residual anomalies and exploited the latter to establish the Euler deconvolution maps (**Figure 8**).

We assigned several values of structural index for the choice of clustering and extension of Euler sources; a parameter that depends on the geometry of the source and characterizes the rate of change of the anomaly intensity with distance. We found that, for a structural index N = 0, a significant clustering of Euler solutions was obtained.

In addition, the highlighted Euler deconvolution maps reveal the shallow and deep contacts and clearly define the depth solutions for the gravity anomalies respectively. The Euler deconvolution map shows a strong dominance of deep geological structures located in the transition zone between the Congo Craton and the Pan-African Ridge; and in the Yoko locality along the ENE-WSW direction with an extension into the Bafia locality. This map also shows that the depths of NE-SW geological structures are between 3 km and 11 km. These structures are limited by a termination at the northern boundary of the Congo Craton in southern Cameroon (Figure 8).

In this work, the structural characterization of the study area is done in the Yaounde - Yoko area including the Sanaga Fault. Due to the resolution of the XGM 2016 global gravity model data used (0.1˚ × 0.1˚), a limited number of lineaments, which were widely spaced apart were located (Figure 7(a)). A comparative analysis with the Euler deconvolution map shows that the study area is marked by the presence of geological structures of varying depths marking the trace of several other structures whose lineaments have not been located; in particular, those marking the presence of the Sanaga fault until the northern termination

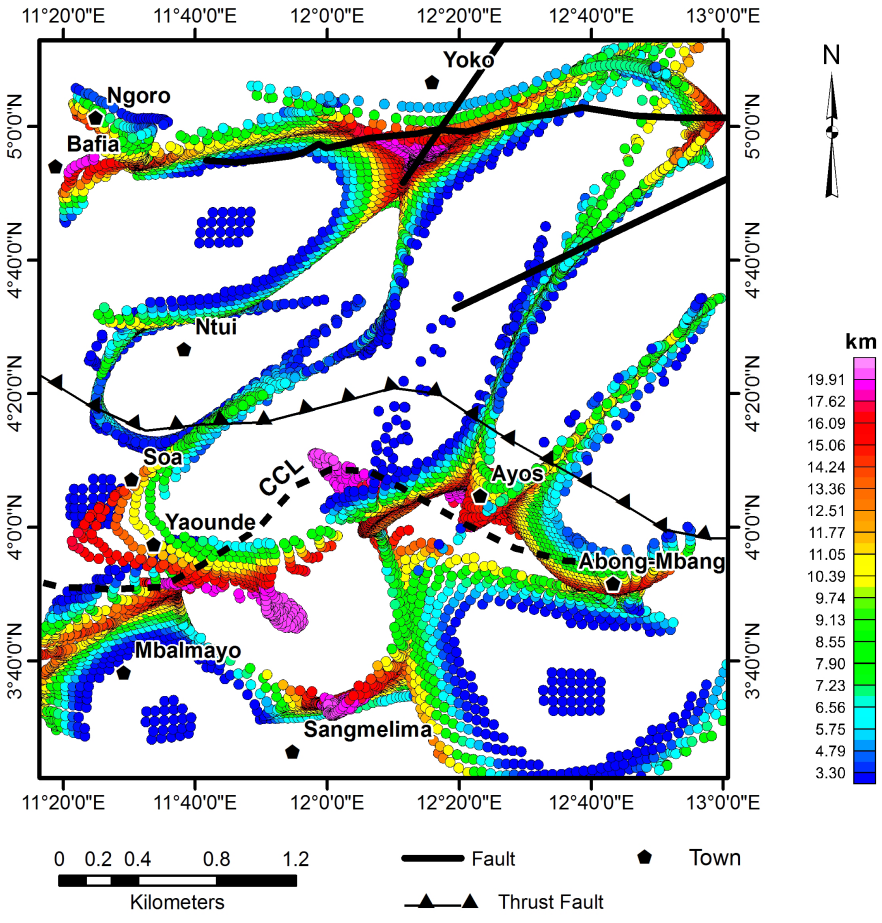

Figure 8. Euler deconvolution map of Bouguer anomalies. Structural index N = 0; tolerance Z = 0 and window 15 km × 15 km. The contour in broken line of brown color indicates the major direction of geological structures marking the trace of Sanaga fault.

with the Congo Craton. This could be due to the different digital filters used governing each method used. The characteristic orientation of the different gravity lineament segments has been located are listed in Table 2.

The rose of representative diagrams was highlighted in order to locate the directions and orientations of the localized gravity lineaments (Figure 9).

The lineaments thus highlighted reveal that the subsurface of the study area is characterized by unknown intracrustal geodynamic processes given the seismic

Table 2. Characteristic orientation of the different segments of gravimetric lineaments.

Lineaments	*Directions*	*Lineaments*	*Directions*	*Lineaments*	*Directions*
F1	N90˚E	F8	N67.5˚E	F15	N90˚E
F2	N78.75˚E	F9	N67.5˚E	F16	N78.75˚E
F3	N33.75˚E	F10	N67.5˚E	F17	N168.75˚E
F4	N67.5˚E	F11	N67.5˚E	F18	N45˚E
F5	N135˚E	F12	N135˚E	F19	N33.75˚E
F6	N135˚E	F13	N56.25˚E		
F7	N90˚E	F14	N101.25˚E		

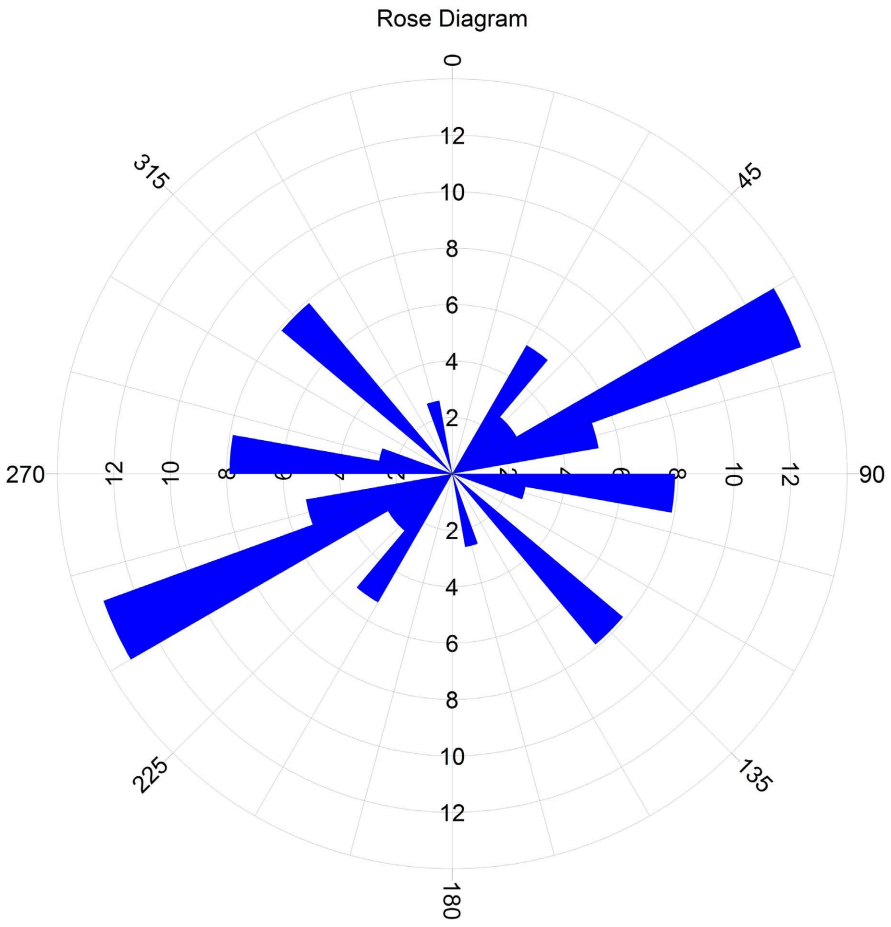

Figure 9. Rose diagram of gravity lineaments revealed by this work.

activities already recorded in the area; in agreement with the hypothesis of [5] and the results of the work of [45]. In the Yaounde locality, a little further south, the lineaments (F11 and F15) located represent the trace of the northern edge of the Congo Craton with the Pan-African Range. In the northern part of the study area, specifically in the locality of Yoko, several lineaments (F1, F8, F14, and F2) are observed, aligning with the tectonic fault indicated by the geological investigations (**Figure 7(a)** & **Figure 7(b)**). In comparison with the geological parameters, these localized lineaments are entirely located on Neoproterozoic granitoids (**Figure 1**). As for the Sanaga Fault, as localized by geological works, the trace of this tectonic accident is also localized in this work by the NE-SW trending lineament F19 located on the Gneiss and micaschists, schists and granitoids (**Figure 1**). Overall, the localized lineaments are evidence that the subsurface of the investigation area is constantly active.

5.8. 2D1/2 Modeling of Gravity Data

5.8.1. Choice of Profiles and Depths of Investigation

The 2D1/2 modeling is done in this work in order to characterize the geometry of the Yaoundé -Yoko basement. The modeling approach employed in this study involves representing the structures as prisms with polygonal cross-sections and infinite elongation. This approach is based on the initial assumption of these structures. In cases where the transverse extension ratios are small, the direct 2D1/2 modeling method considers the limited length of the geological body [39]. Between these two localities, two large extensions of major positive anomalies are located, the first in the center following the NE-SW direction which, according to geology, marks the presence of the Sanaga fault. The second is north of Ntui, indicating the presence of a rock intrusion. However, we chose five profiles (AA', BB', CC', DD' and EE') with a North-South direction (**Figure 10**), crossing these two localities and also including the anomalies characteristic of the Sanaga Fault. Furthermore, the choice of the depth of investigation was made following the qualitative analysis from the upward extension. We took into account the observations made during the multiscale analysis of the Bouguer anomalies (**Figure 4**) which shows us that the strong contrasts of characteristic anomalies of the Sanaga Fault with depth disappear at 30 - 40 km. For our models, the depth of investigation was set at 45 km. The selection of the depth in our study was determined through a qualitative analysis, particularly by extending upwards. In the study region, the depth of the Moho, which represents the boundary between the crust and mantle, has been estimated at 43 km [46] and 40 km [40]. For our modeling purposes, we fixed this depth at 45km within the mantle.

5.8.2. Choice of Densities and Contrasts

We have seen during the analysis that a heavy anomaly (positive) denotes the existence at depth of materials denser than normal and that a light anomaly characterizes at depth materials less dense than normal. In this section, our focus is solely on the density of rocks incorporated in our models [47]. The final model

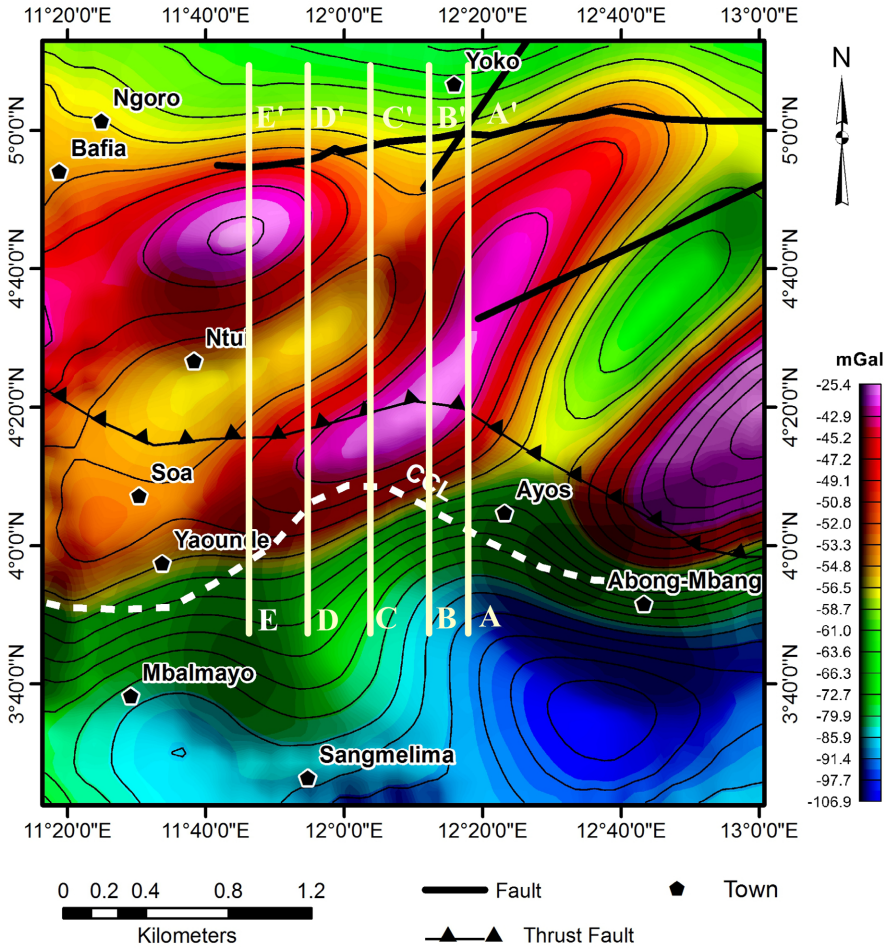

Figure 10. Bouguer anomaly map showing profile positions.

was derived by adjusting the volume of density blocks representing geological structures. Only contrast values that resulted in the best match between the calculated theoretical curve and the experimental curve were considered for density determination. These contrasts are calculated with respect to a density $d_0 = 2.67$ g/cm^3 taken as reference which is in principle that of the earth's crust. **Figures 11-15** illustrate the results of the models thus highlighted.

5.8.3. Models Gravity Data Interpretation

The interpretation here is done along five gravity profiles (AA', BB', CC', DD' and EE'), oriented S-N, all almost perpendicular to the Bouguer anomaly contours and a length of about 157 km. These gravity profiles are plotted from the Bouguer anomaly map and used to build the 2D1/2 models (**Figures 11-15**). From our models, 8 blocks of geological structures of different densities were located; except for the CC' profile, which presents 7 blocks of different densities. The models (**Figures 11-15**) reveal that the positive anomaly located on the Sanaga fault reflects the anomalous character due to the presence of the Schist intrusion in the basement. North of Ntui, the basement is characterized by the presence of granulite rocks, granites and the intrusion of Gneiss (**Figure 1**).

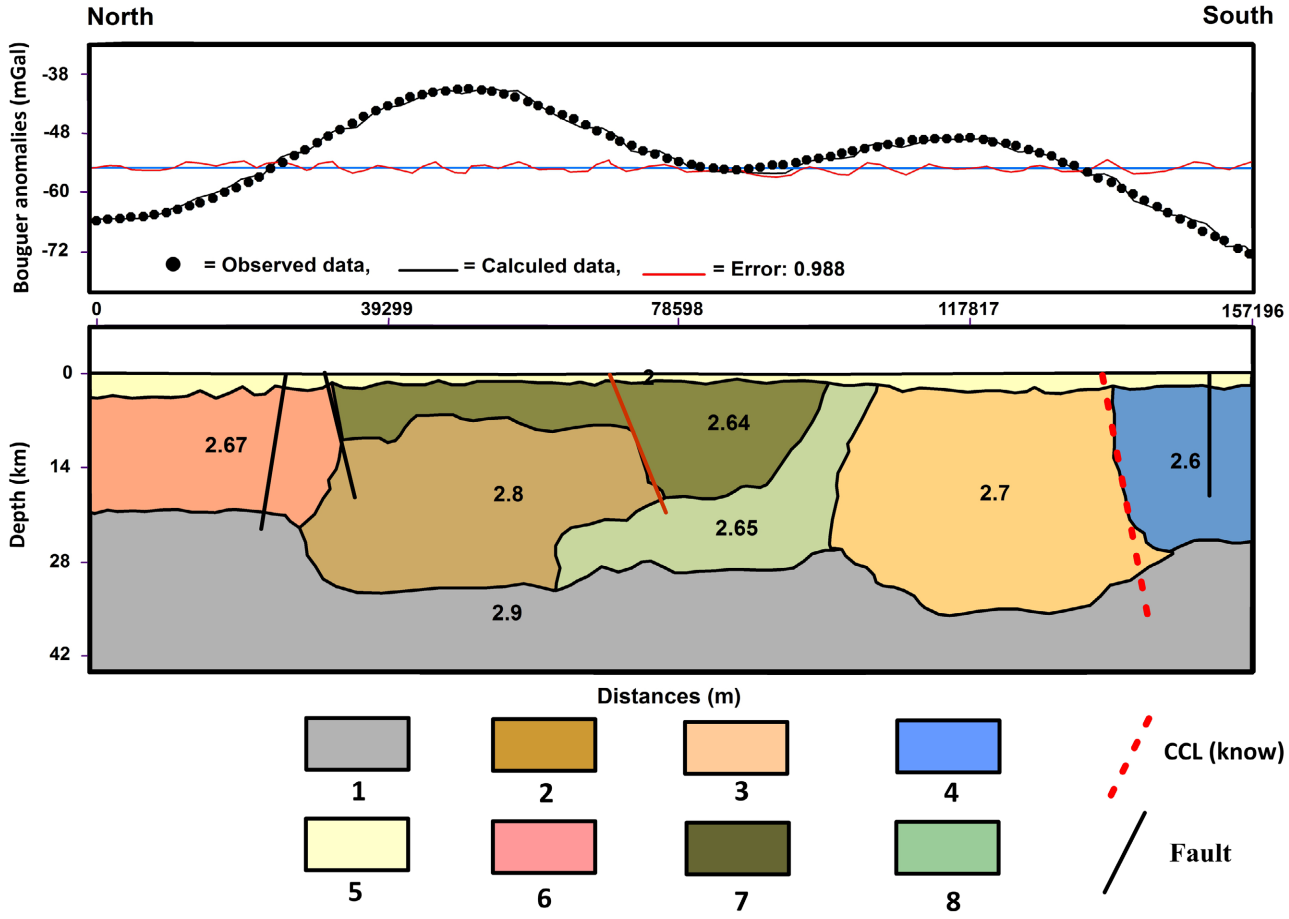

Figure 11. Illustration model profil AA'; 1. Lower crust d1 = 2.9 g/cm^3; 2. Gneiss d2 = 2.8 g/cm^3; 3. Schistes d3 = 2.7 g/cm^3; 4. Crust granites de So'o (Congo Craton) d4 = 2.6; 5. Sedimentary rock d5 = 2 g/cm^3; 6. Granites Syntectonics d6 = 2.67 g/cm^3. 7. Granulites d7 = 2.64 g/cm^3; 8. Granites d8 = 2.65 g/cm^3.

South of the profiles, the models show an outcrop of the Congo Craton crust. The border of this crust with the Pan-African Range, marks the presence of two constraints: 1) the N-W thrust of the shale from the North Equatorial Pan-African Range by the Congo Craton (Figure 11 and Figure 12); 2) and the thrust of the cratonic crust by the Pan-African Range (Figure 12, Figure 14 and Figure 15). The faulted contacts (CCL) So'o schists-granite (Congo Craton), So'o sandstone-granite (Congo Craton) with strong density contrast are responsible for the strong gradient observed on all profiles and mark the discontinuity between the Pan-African Range and the Congo Craton.

In the locality of Yoko, the main formation is that associated with the Syntectonic granites. It outcrops and is in contact with the gneiss. It is responsible for the relative minimum anomaly observed to the north of the profile. Moreover, we note quasi-oscillatory variations in the density contrast of the bedrock (gneiss, granulites, granits) in relation to the host (crust) on all models. These variations have confirmed the heterogeneity of the bedrock and the thinning of the bedrock. This heterogeneity would be due to the upwelling of denser materials from the upper mantle into the crust. We observe an overflow of the

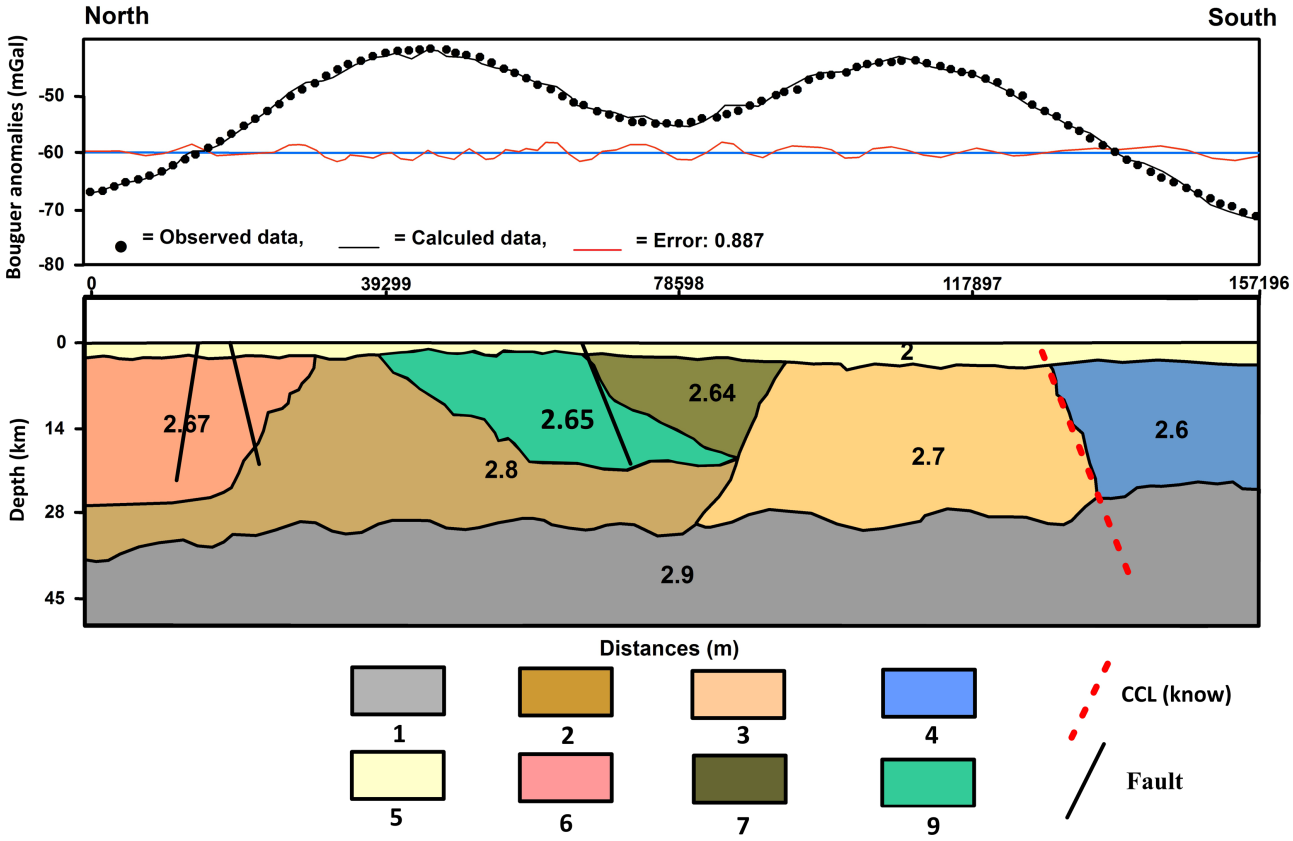

Figure 12. Illustration model profil BB'; 1. Lower crust d1 = 2.9 g/cm^3; 2. Gneiss d2 = 2.8 g/cm^3; 3. Schistes d3 = 2.7 g/cm^3; 4. Crust granites de So'o (Congo Craton) d4 = 2.6; 5. Sedimentary rock d5 = 2 g/cm^3; 6. Granites Syntectonics d6 = 2.67 g/cm^3. 7. Granulites d7 = 2.64 g/cm^3; 9. Granites d9 = 2.65 g/cm^3.

Pan-African chain formations (sandstones, shales) on those of the Congo Craton (So'o granites).

Overall, the 2D1/2 models also show that the subsurface of the Yaounde - Yoko area are characterized by a variety of geological structures of different densities reflecting a complex geodynamic context. This observation highlights the significance of recognizing that the subsoil in the study area may potentially host multiple geodynamic mechanisms, likely originating from the mantle.

6. Discussion

In this study the subsurface of Yaounde - Yoko area for structural characterization of the subsurface. First, as results, some lineament networks are highlighted from the multi-scale analysis of anomalies and gradient contrasts of the global gravity model XGM2016 for extensional altitudes up to 35 km. Important geophysical investigations have been directed in the structural analysis of the Cameroonian basement [2] [7] [43] [44] in order to propose the directions of its tectonic faults. The results of the studies by these authors have led to the structuring of a set and main litho-tectonic units on the Pan-African Range and the cratonic part; these are: the Central Cameroon Shear (CCC), the Foumban-Tibati-Banyo fault (FFTB) [7] which is a ductile fault [4] [5] [45], the Bétaré-Oya Fault (BOF)

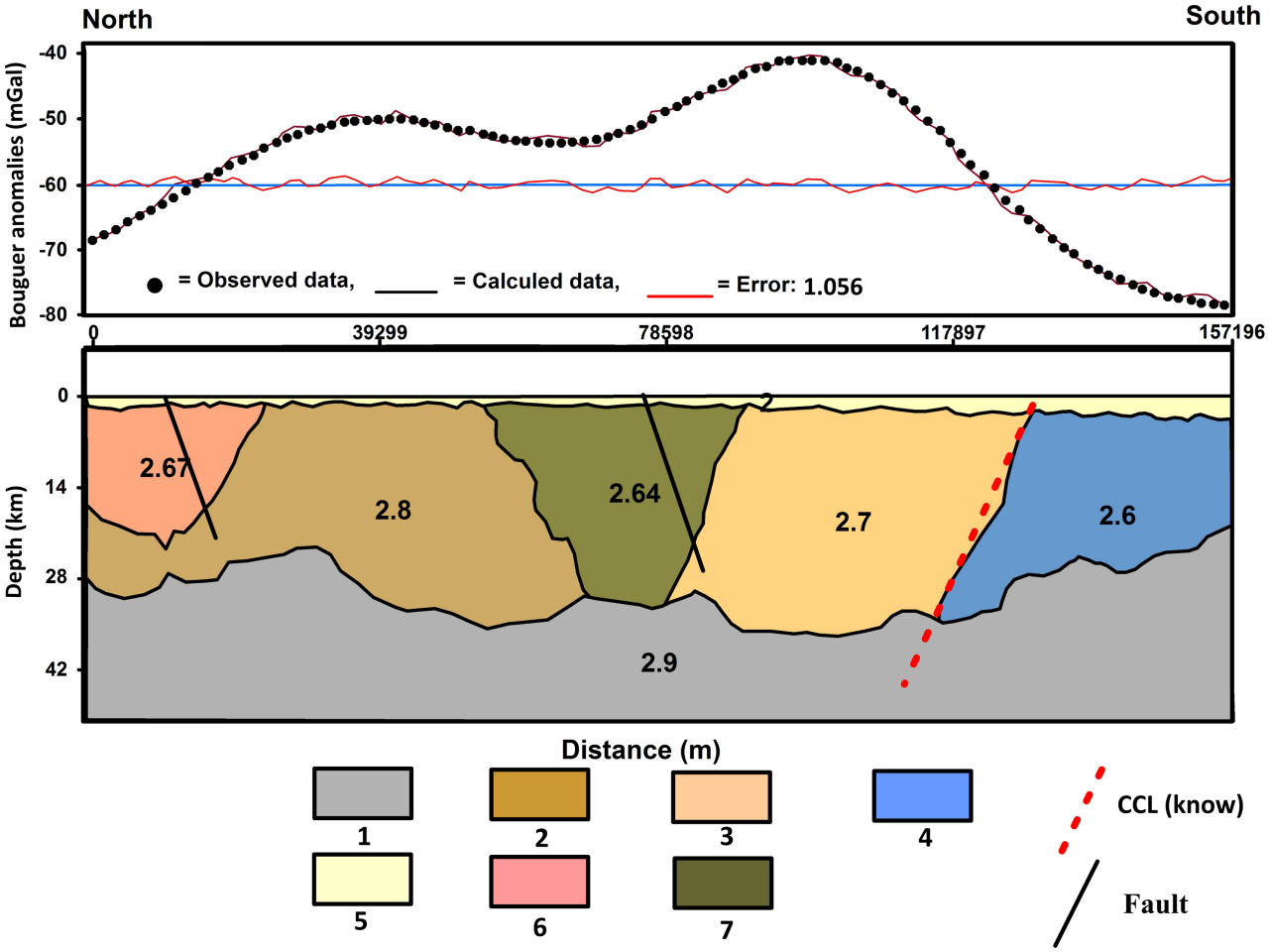

Figure 13. Illustration model profil CC'; 1. Lower crust d1 = 2.9 g/cm^3; 2. Gneiss d2 = 2.8 g/cm^3; 3. Schistes d3 = 2.7 g/cm^3; 4. Crust granites de So'o (Congo Craton) d4 = 2.6; 5. Sedimentary rock d5 = 2 g/cm^3; 6. Granites Syntectonics d6 = 2.67 g/cm^3. 7. Granulites d7 = 2.64 g/cm^3.

which is a ductile-fragile fault and the Sanaga Fault [45]. The lineaments located in this work confirm the presence of some structural features already located in the past. In the study area, the structural trace of the Sanaga fault was located by [2]. The lineaments thus located in this work, confirm the emplacement of the Sanaga fault; in agreement with [5] on the Sanaga Fault activity.

The work of [2] [10] in the study of the geodynamics of the Pan-African Range showed that the northern edge of the Congo Craton in the southern part of Cameroon is the result of a continental collision. This could explain the presence of gradient contrasts in the Abong-Mbang locality in the direction of Yaoundé, also involving that characterizing the Sanaga fault. According to the Euler deconvolution map, the Sanaga Fault is located between two linear arrays of deep geological structures and would be permanently subjected to compressive stress; this could be in agreement with the hypothesis of [5] who revealed that the Sanaga Fault is active due to geodynamic stress.

In addition, work on the Source characterization and tectonic implications of the M4.6 Monatélé (Cameroon) earthquake of 19 March 2005 by [39], analyzed

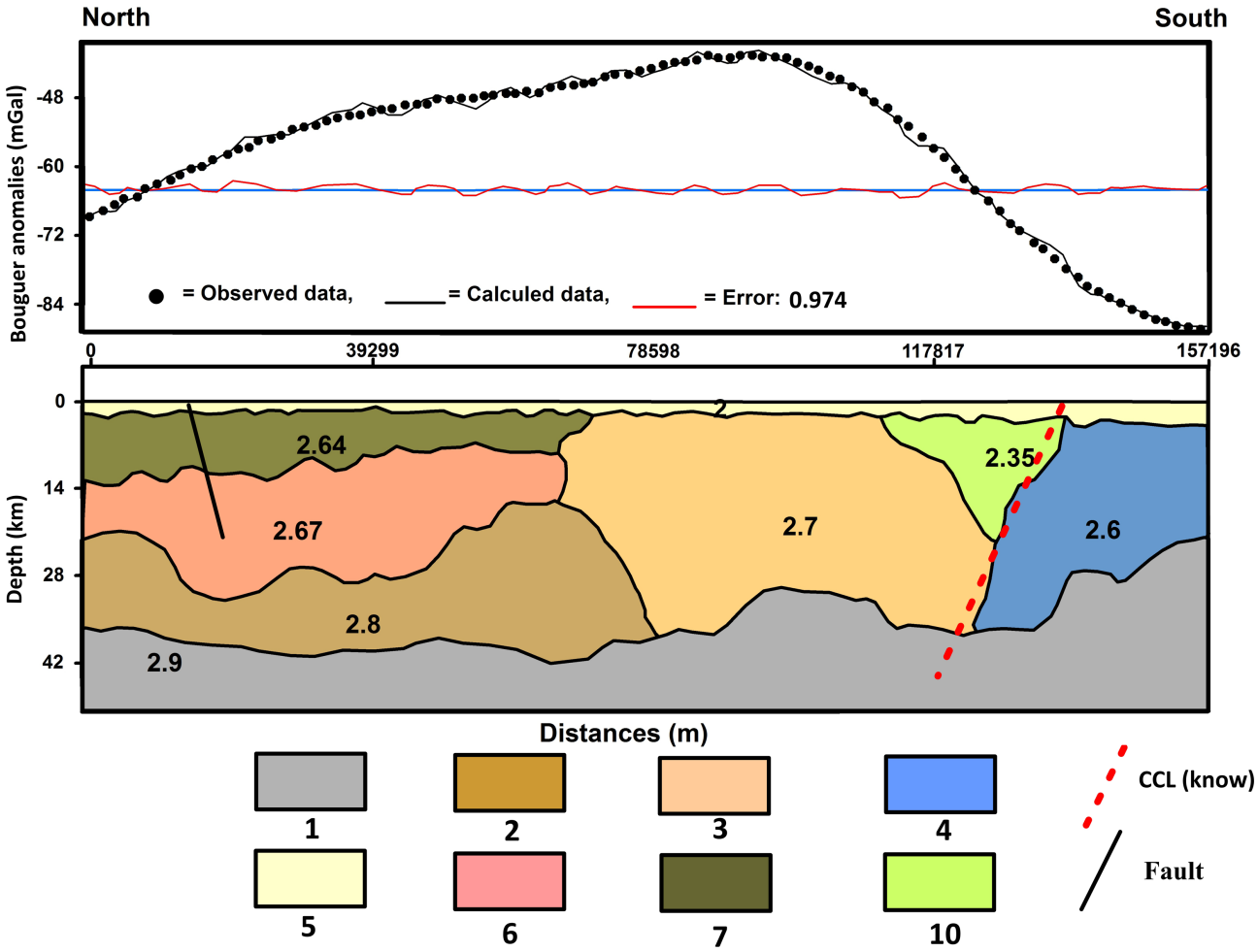

Figure 14. Illustration model profil DD'; 1. Lower crust d1 = 2.9 g/cm^3; 2. Gneiss d2 = 2.8 g/cm^3; 3. Schistes d3 = 2.7 g/cm^3; 4. Crust granites de So'o (Congo Craton) d4 = 2.6; 5. Sedimentary rock d5 = 2 g/cm^3; 6. Granites Syntectonics d6 = 2.67 g/cm^3. 7. Granulites d7 = 2.64 g/cm$^{3;}$ 10. Grès d10 = 2.35 g/cm^3.

broadband seismograms recorded by the Cameroon regional network to locate the event and determine the source mechanism in the area. Correlation of the seismicity with gravity data allowed us to study the seismotectonic implications and show that the epicenter is located near the northeast segment of the Sanaga Fault; with an intra-crustal focal depth of 11 km [39]. The investigation on the imaging of the crustal structures of the basement of South Cameroon and their implications on tectonics from qualitative and quantitative approaches allowed to characterize the crustal structures in this region and to trace the evolution of the Congo Craton [43]. Also, mapping of the tectonic lineaments of Cameroon from potential field data [7] have allowed for the global structuring of characteristic tectonic faults in the subsurface. This work has allowed us to understand that the geological structures of the basement of Yaounde, Yoko area in Sud-Cameroon are affected by tectonic activities where the processes responsible for them are still poorly understood. The results obtained in this work are in agreement with the results of these authors.

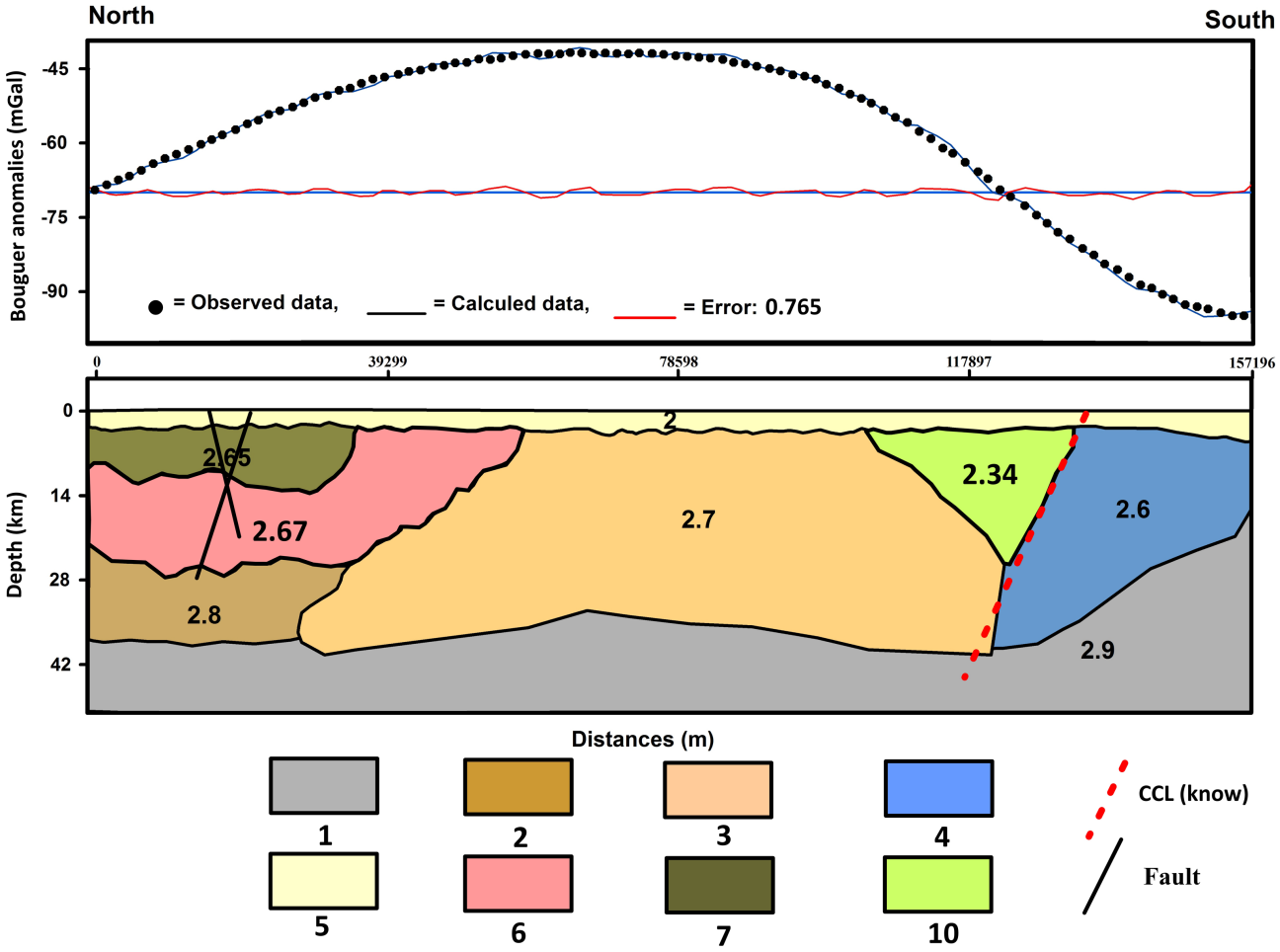

Figure 15. Illustration model profil EE'; 1. Lower crust d1 = 2.9 g/cm^3; 2. Gneiss d2 = 2.8 g/cm^3; 3. Schistes d3 = 2.7 g/cm^3; 4. Crust granites de So'o (Congo Craton) d4 = 2.6; 5. Sedimentary rock d5 = 2 g/cm^3; 6. Granites Syntectonics d6 = 2.67 g/cm^3. 7. Granulites d7 = 2.64 g/cm$^{3;}$ 10. Grès d10 = 2.35 g/cm^3.

Secondly, 2D1/2 modeling of the subsurface geological structures of the Yaounde - Yoko localities was done in order to characterize the intracrustal geometry of the area. These models show that the basement of the study area is characterized by a number of geological structures of different densities. These structures present complex shapes marking the trace of geodynamic processes responsible for their deformations. In the area where the Sanaga Fault is located, a shale intrusion has been located. The geology of the study area shows us a spatial distribution of this structure in the subsurface of this area. Thus our proposed models are in agreement with the geology of the investigated area and integrate the presence of geological structures already evidenced by geological works.

The analysis of anomalies derived from the global gravity model (XGM2016) indicates that the basement, which includes the Sanaga fault near Yaounde-Yoko in Southern Cameroon, exhibits intricate gravity patterns. However, the resolution of the XGM2016 data limits the identification of lineaments in the region. Nevertheless, the presence of complex gravity gradients suggests that localized

geological structures in the basement are continually influenced by various geodynamic forces and constraints. This corroborates the results of [5] who showed that the Sanaga fault is active; in accordance with work of Ngatchou [48].

7. Conclusions

In this work, data from the XGM2016 global gravity model are used to investigate the subsurface of Yaoundé - Yoko. The main objective was to investigate the basement of these localities in order to locate the characteristic tectonic faults in the study area. For the analysis, several transformation methods such as upward extension, vertical and horizontal gradients were exploited for a qualitative analysis of the Bouguer anomalies and their gradient contrasts. The qualitative interpretation of the Bouguer anomalies revealed that the investigation area is characterized by two major axes of anomalies along the ENE-WSW and NE-SW directions. A correlation of these anomalies with the geology of the study area shows that the major positive NE-SW trending anomalies may correspond to the Sanaga Fault.

For the quantitative analysis, the Euler deconvolution method is used to highlight the spatial distribution of the depths of geological structures in the study area. In addition, a multiscale analysis of Bouguer anomalies and their gradients was performed to map the tectonic faults characteristic of the basement in the investigation area. As a result, considering the sampling step of the data, the lineaments thus located show less importance. However, from this map, it was possible to identify the structural features representing the northern limit of the Congo Craton with the Pan-African Chain; located between Abong-Mbang and Ayos, going towards Yaounde in an East-West direction. Through the study of the basement structures of the Pan-African Range in the region, the continent-to-continent collision model involving the Congo Craton and the active edge of north-central Cameroon showing Archean to Paleoproterozoic legacies was proposed [2].

This collision phenomenon could be one of the factors responsible for the strong presence of gravity lineaments and discontinuities observed in particular the Sanaga Fault (SF) as well as those of the northern and western edges between the Pan-African Range and the Congo Craton. Five N-S profiles were chosen for the 2D1/2 modeling. The results thus obtained highlight the presence of eight geological structures of different densities; among which the granulite and granitic intrusions are to the north of the profiles and the schist intrusion is to the south of the profiles. Our models also highlight a fracture (So'o schist-granite contact) located to the south that seems to have favored on the one hand the thrust of the geological structures of the Pan-African Range outcropping by the So'o cratonic granites; and on the other hand the thrust and ascent of the Pan-African Range on the granites of the Congo Craton. Moreover, the quasi-oscillatory variations of the density contrast of the bedrock (gneiss, granulites, So'o granites) with respect to the surrounding material (crust) on all the models

are highlighted and thus confirm the heterogeneity of the bedrock and the deformation of the structures at the base due to the upwelling of denser materials from the upper mantle into the crust. It also shows that the localized geological structures are permanently subjected to several geodynamic constraints at the origin of the activities of the Sanaga fault.

Acknowledgments

The authors thank the International Centre for Global Earth Models (ICGEM) of the International Gravity Field Service (IGFS) for making available the global gravity model data XGM2016 used in this paper.

Conflicts of Interest

The authors declare no conflicts of interest regarding the publication of this paper.

References

[1] Rolin, P. (1995) La zone de décrochements panafricains des Oubanguides en République Centrafricaine. *Comptes Rendus de l'Académie des Sciences*, **320**, 63-69.

[2] Toteu, S.F., Penaye, J. and Poudjom Djomani, Y. (2004) Geodynamic Evolution of the Pan-African Belt in Central Africa with Special Reference to Cameroon. *Canadian Journal of Earth Sciences*, **41**, 73-85. https://doi.org/10.1139/e03-079

[3] Cornacchia, M. and Dars, R. (1983) Un trait structural majeur du continent Africain; Les linéaments centrafricains du Cameroun au Golfe d'Aden. *Bulletin de la Société Géologique de France*, **S7-XXV**, 101-109. https://doi.org/10.2113/gssgfbull.S7-XXV.1.101

[4] Nzenti, J.P., Barbey, P., Macaudière, J. and Soba, D. (1988) Origin and Evolution of the Late Precambrian High-Grade Yaounde Gneisses (Cameroon). *Precambrian Research*, **38**, 91-109. https://doi.org/10.1016/0301-9268(88)90086-1

[5] Dumont, J.F. (1986) Identification par télédétection de l'accident de la Sanaga (Cameroun). Sa position dans le contexte des grands accidents d'Afrique centrale et de la limite nord du craton congolais. *Géodynamique*, **1**, 13-19.

[6] Mbom Abane, S. (1997) Investigations géophysiques en bordure du Craton du Congo et implications structurales. Master's Thesis, Université de Yaoundé, Yaoundé.

[7] Cheunteu Fantah, C.A., Mezoue, C.A., Mouzong, M.P., Tokam Kamga, A.P., Nouayou, R. and Nguiya, S. (2022) Mapping of Major Tectonic Lineaments across Cameroon Using Potential Feld Data. *Earth, Planets and Space*, **74**, Article No. 59. https://doi.org/10.1186/s40623-022-01612-7

[8] Boukeke, D.B. (1994) Structures Crustales d'Afrique Centrale Déduites des Anomalies Gravimétriques et Magnétiques: Le Domaine Précambrien de la République Centrafricaine et du Sud Cameroun. Ph.D. Thesis, Université de Paris Sud, Paris.

[9] Vicat, J.P., Pouclet, A. and Nsifa, E. (1998) Les dolérites du groupe du Ntem (Sud Cameroun) et des régions voisines (Centrafrique, Gabon, Congo, Bas-Zaïre). Caractéristiques géochimiques et place dans l'évolution du craton du Congo au Protérozoïque. *Geocam*, **1**, 305-324.

[10] Toteu, S.F., Van Schmus, W.R., Penaye, J. and Michard, A. (2001) New U-Pb and

Sm-Nd Data from North-Central Cameroon and Its Bearing on the Pre-Pan African History of Central Africa. *Precambrian Research*, **108**, 45-73. https://doi.org/10.1016/S0301-9268(00)00149-2

[11] Abdelsalam, M.G., Liégeois, J.P. and Stern, R.J. (2002) The Saharan Metacraton. *Journal of African Earth Sciences*, **34**, 119-136. https://doi.org/10.1016/S0899-5362(02)00013-1

[12] Lassere, M. and Soba, D. (1976) Age libérien des granodiorites et des gneiss à pyroxène du Cameroun méridional. *Bulletin du BRGM*, **2**, 17-32.

[13] Cahen, L., Snelling, N.J., Delhal, J. and Vail, J.R. (1984) The Geochronology and Evolution of Africa. Clarendon Press, Oxford.

[14] Feybesse, J.L., Johan, V., Maurizot, P. and Abessolo, A. (1986) Mise en évidence d'une nappe syn-métamorphe d'âge éburnéen dans la partie Nord-Ouest du craton zaïrois, Sud-Ouest Cameroun. In: *Les formations birrimiennes en Afrique de l'Ouest. Compte rendu de conférences*, Occasional Publications-CIFEG, Orléans, 105-111. http://pascal-francis.inist.fr/vibad/index.php?action=getRecordDetail&idt=8040889

[15] Toteu, S.F., Penaye, J., Maldan, F., Nyama Atibagoua, B., Bouyo Houketchang, M. and Sep, J.P. (2008) Nlomgan, Géologie et ressources minérales du Cameroun. 33*eme congrès International de la Géologie*, Oslo, 6-14 August 2008.

[16] Nédelec, A., Macaudière, J., Nzenti, J.P. and Barbey, P. (1986) Evolution structural et métamorphique de la série de Mbalmayo (Cameroun): Implications pour la structure de la zone mobile panafricaine au contact du craton du Congo. *C.R. Académie des Sciences Paris*, **303**, 75-80.

[17] Bessoles, B. and Trompette, R. (1980) Géologie d'Afrique. La chaîne panafricaine, zone mobile d'Afrique centrale (partie sud) et zone soudanaise. Mémoires du Bureau de recherches géologiques et minières, Orléans.

[18] Zingerle, P., Brockmann, J.M., Pail, R., Gruber, T. and Willerg, M. (2019) The Polar Extended Gravity Field Model TIM_R6e. GZF Data Services.

[19] Uieda, L. and Barbosa, V.C. (2017) Fast Nonlinear Gravity Inversion in Spherical Coordinates 849 with Application to the South American Moho. *Geophysical Journal International*, **208**, 162-176. https://doi.org/10.1093/gji/ggw390

[20] Hinze, W.J. (2003) Bouguer Reduction Density, Why 2.67? *Geophysics*, **68**, 1559-1560. https://doi.org/10.1190/1.1620629

[21] Tenzer, R., Vajda, P. and Hamayun, P. (2010) A Mathematical Model of the Bathymetry Generated External Gravitational Field. *Contributions to Geophysics and Geodesy*, **40**, 31-44. https://doi.org/10.2478/v10126-010-0002-8

[22] Tenzer, R., Novák, P. and Gladkikh, V. (2011) On the Accuracy of the Bathymetry-Generated Gravitational Field Quantities for a Depth-Dependent Seawater Density Distribution. *Studia Geophysica et Geodaetica*, **55**, 609-626. https://doi.org/10.1007/s11200-010-0074-y

[23] Tenzer, R., Pavel, N. and Vladislav, G. (2012) The Bathymetric Stripping Corrections to Gravity Field Quantities for a Depth-Dependent Model of Seawater Density. *Marine Geodesy*, **35**, 198-220. https://doi.org/10.1080/01490419.2012.670592

[24] Gladkikh, V. and Tenzer, R. (2012) A Mathematical Model of the Global Ocean Saltwater Density Distribution. *Pure and Applied Geophysics*, **169**, 249-257. https://doi.org/10.1007/s00024-011-0275-5

[25] Cordell, L. and Grauch, V.J.S. (1985) Mapping Basement Magnetization Zones from

Aeromagnetic Data in the San Juan Basin, New Mexico. In: Hinze, W.J., Ed., *The Utility of Regional Gravity and Magnetic Anomaly Maps*, Society Exploration Geophysicists, Tulsa, 181-197. https://doi.org/10.1190/1.0931830346.ch16

[26] Blakely, R.J. and Simpson, R.W. (1985) Approximating Edges of Source Bodies from Magnetic or Gravity Anomalies. *Geophysics*, **51**, 1494-1498. https://doi.org/10.1190/1.1442197

[27] Everaerts, M. and Mansy, J.L. (2001) Le filtrage des anomalies gravimétriques, une clé pour une compréhension des structures tectoniques du Boulonnais et de l'Artois (France). *Bulletin de la Société Géologique de France*, **172**, 267-274. https://doi.org/10.2113/172.3.267

[28] Khattach, D., Keating, P., Mostafa, M.L., Chennouf, T., Andrieux, P. and Milhi, A. (2004) Apport de la gravimétrie à l'étude de la structure du bassin des Trifa (Maroc nord-oriental): Implications hydrogéologiques. *Comptes Rendus Geoscience*, **336**, 1427-1432. https://doi.org/10.1016/j.crte.2004.09.012

[29] Jacobsen, B.H. (1987) A Case for Upward Continuation as a Standard Separation Flter for Potential-Feld Maps. *Geophysics*, **52**, 390–398. https://doi.org/10.1190/1.1442378

[30] Florio, G., Fedi, M. and Pasteka, R. (2006) On the Application of Euler Deconvolution to the Analytic Signal. *Geophysics*, **71**, 87-93. https://doi.org/10.1190/1.2360204

[31] Koumetio, F., Njomo, D., Tabod, C.T., Noutchogwe, T.C. and Manguelle-Dicoum, E. (2012) Structural Interpretation of Gravity Anomalies from the Kribi—Edea Zone, South Cameroon: A Case Study. *Journal of Geophysics and Engineering*, **9**, 664-673. https://doi.org/10.1088/1742-2132/9/6/664

[32] Noutchogwe, C.B. (2010) Investigation géophysique dans la région de l'Adamaoua par les méthodes gravimétriques et magnétiques: implications structurales et hydrologiques. Master's Thesis, Université de Yaoundé I, Yaoundé.

[33] Reid, A.B., Allsop, J.M., Granser, H., Millet, A.J. and Somerton, I.W. (1990) Magnetic Interpretation in Three Dimensions Using Euler Deconvolution. *Geophysics*, **55**, 180-191. https://doi.org/10.1190/1.1442774

[34] Thomson, D.T. (1982) EULDPH: A New Technique for Making Computer-Assisted Depth Estimates from Magnetic Data. *Geophysics*, **47**, 31-37. https://doi.org/10.1190/1.1441278

[35] Marson, I. and Klingele, E.E. (1993) Advantages of Using the Vertical Gradient of Gravity for 3-D Interpretation. *Geophysics*, **58**, 1588-1595. https://doi.org/10.1190/1.1443374

[36] Hatem, A. and Mostafa, R. (2013) Delineation of the Subsurface Structures and Basement Surface of the Abu-Rodaym Area, South Western Sinai, Using Ground Magnetic Data. *Earth, Planets and Space*, **65**, 749-757. https://doi.org/10.5047/eps.2012.12.006

[37] Stavrev, P.Y. (1997) Euler Deconvolution Using Differential Similarity Transformation of Gravity or Magnetic Anomalies. *Geophysical Prospecting*, **45**, 207-246. https://doi.org/10.1046/j.1365-2478.1997.00331.x

[38] Cady, J.W. (1980) Calculation of Gravity and Magnetic Anomalies of Finite Length Right Polygonal Prisms. *Journal of Geophysical Research*, **45**, 1507-1512. https://doi.org/10.1190/1.1441045

[39] Shuey, R.T. and Pasquale, A.S. (1973) End Corrections in Magnetic Profile Interpretation. *Geophysics*, **38**, 507-512. https://doi.org/10.1190/1.1440356

[40] Cheunteu Fantah, C.A., Tokam Kamga, A.P., Mouzong, M.P., Nouayou, R. and Nguiya, S. (2023) Structure of Lithosphere Beneath Cameroon Using Global Gravity Model Data: Implications for the Setting of the Cameroon Volcanic Line. *Acta Geophysica*.

[41] Tadjou, J.M., Nouayou, R., Kamguia, J., Kande, H.L. and Manguelle-Dicoum, E. (2009) Gravity Analysis of the Boundary between the Congo Craton and the Panafrican Belt of Cameroon. *Austrian Journal of Earth Sciences*, **102**, 71-79.

[42] Shandini, Y., Kouske, A.P., Nguiya, S. and Mouzong, P.M. (2018) Structural Setting of the Koum Sedimentary Basin (North Cameroon) Derived from EGM2008 Gravity Feld Interpretation. *Contributions to Geophysics and Geodesy*, **48**, 281-298. https://doi.org/10.2478/congeo-2018-0013

[43] Nguiya, S., Cheunteu Fantah, C.A. and Nouayou, R. (2018) Gravity Imaging of the Crustal Structures Beneath Southern Cameroon and Its Tectonic Implications. *The International Journal of Engineering and Science*, **78**, 8-23.

[44] Owona Angue, M.L.C., Tabod, C.T., Nguiya, S., Kenfack, J.V. and Tokam A.P. (2013) Kamga, Delineation of lineaments in South Cameroon (Central Africa) Using Gravity Data. *Open Journal of Geology*, **3**, 331-339. https://doi.org/10.4236/ojg.2013.35038

[45] Kankeu, B. (2008) Anisotropie de la susceptibilité magnétique (ASM) et fabriques des roches Néoprotérozoiiques des régions de Garga-Sarali et Bétaré-Oya à l'Est Cameroun: Implications géodynamiques pour l'évolution de la chaîne panafricaine d'Afrique Centrale. Ph.D. Thesis, Université de Yaoundé I, Yaoundé.

[46] Tokam, K.A.P., Tabod, C.T., Nyblade, A.A., Julia, J., Wiens, D.A. and Pasyanos, M. (2010) Structure of the Crust beneath Cameroon, West Africa, from the Joint Inversion of Rayleigh Wave Group Velocities and Receiver Functions Geophysical. *Geophysical Journal International*, **1183**, 1061-1076. https://doi.org/10.1111/j.1365-246X.2010.04776.x

[47] Telford, W.M., Geldart, L.P. and Sheriff, R.E. (1990) Applied Geophysics. 2nd Edition, Cambridge University Press, Cambridge. https://doi.org/10.1017/CBO9781139167932

[48] Ngatchou, H.E., Nguiya, S., Owona Angue, M.L.C., Mouzong, P.M. and Tokam, A.P. (2018) Source Characterization and Tectonic Implications of the M4.6 Monatélé (Cameroon) Earthquake of 19 March 2005. *South African Journal of Geology*, **121**, 191-200. https://doi.org/10.25131/sajg.121.0015